3D THINNING AND ITS APPLICATIONS TO MEDICAL IMAGE PROCESSING

KÁLMÁN PALÁGYI[1], ERICH SORANTIN[2],
CSONGOR HALMAI[1] AND ATTILA KUBA[1]

[1]*Department of Applied Informatics, Jozsef Attila University, H–6701 Szeged P.O. Box 652, Hungary*
palagyi@inf.u–szeged.hu

[2]*Department of Radiology, Karl Franzens University, Auengruggerplatz 34, A–8036, Graz, Austria*

Abstract: Skeleton is a frequently used feature to represent general form of an object. The importance of that region–based shape feature shows an upward tendency in medical image processing, too. This paper summarizes the major skeletonization approaches, the parallel thinning methodologies in 3D, and some emerged medical applications. An application to calculate the cross–sectional profiles of blood vessels is also presented.

Keywords: skeletonization techniques, 3D parallel thinning, medical image processing

1. Skeleton and skeletonization techniques

The notion of *skeleton* was introduced by Blum [3] as the result of the Medial Axis Transform. It is a region–based shape feature/descriptor, which summarizes the general form of objects/shapes. A very illustrative definition of the skeleton is given using the prairie–fire analogy: the object boundary is set on fire and the skeleton is formed by the loci where the fire fronts meet and quench each other. This definition can be naturally extended to any dimension. In the 2D/3D Euclidean space, the skeleton is the locus of the centers of all maximal inscribed disks/balls. Note that maximal inscribed nD hyperspheres are to be considered in nD. The equivalence of the "meeting points" of the prairie–fire and the centers of maximal inscribed hyperspheres has been proved by Calabi and Hartnett [7]. The continuous skeleton of a solid 3D box is illustrated in Figure 1.

There are two major methods for shape representation. The first method describes the boundary that surrounds an object. The second one gives

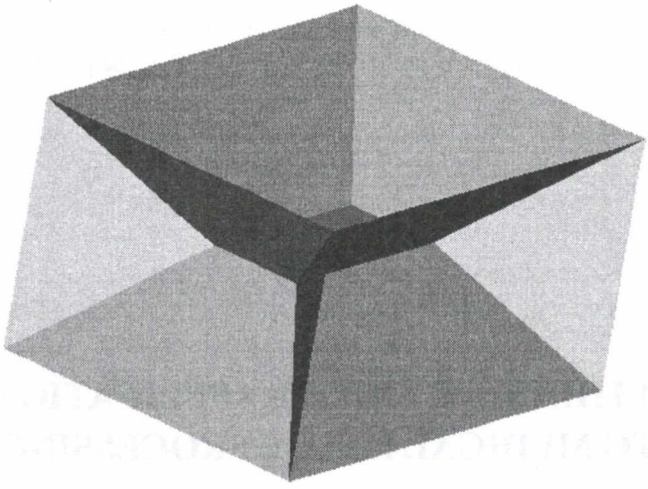

Figure 1. *Skeleton of a (3D) solid box*

a representation of the region that is occupied by the object to be analyzed. Boundary–based techniques are widely used but there are some deficiencies which limit their usefulness in practical applications, especially in 3D [29]:

— methods of differential geometry are rather sensitive to noise;

— occlusion may seriously disturb boundary–based descriptors;

— they are not appropriate to extract global shape features and to make them explicit;

— they can rather insufficiently reveal the hierarchical organization of the shape.

The concept of *skeletonization* (i.e., skeleton extraction from discrete binary images) should be able to help exactly at the points listed above. The local object symmetries represented by the skeleton certainly cannot replace boundary–based shape descriptors, but complement and support them.

During the last two decades skeletonization has become a challenging research field. There are two major requirements to be complied with [29]. The first one is *geometrical*. It means that the skeleton must be in the "middle" of the object and invariant under geometrical transformations including translation, rotation, and scaling. The second one is *topological* requiring the produced skeleton to be topologically equivalent to the original object.

Three major discrete skeletonization methods have been proposed:

— using distance transformation;

— extracting from Voronoi–diagram;

— thinning.

The first method is to find the maximal inscribed hyperspheres. It requires the following 3–step process:

1. The original binary picture is converted into another one containing feature and non–feature elements, where feature elements belong to the boundary of the discrete object.
2. The *distance map* is generated where each element has a value that approximates the distance to the nearest feature element [4].
3. Local maxima or ridges in the distance map are detected as skeletal points.

The result of the distance transformation depends on the selected distance and the ridge extraction is a rather difficult task. The distance map based method fulfils the geometrical requirement if a good approximation to the Euclidean distance is applied, but the topological correctness is not guaranteed.

The *Voronoi diagram* of a discrete set of points (called generating points) is the partition of the given space into cells so that each cell contains exactly one generating point and the locus of all points which are nearer to this generating point than to other generating points. It has been shown that the skeleton of an object which is described by a set of boundary points can be approximated by a subgraph of the Voronoi diagram of that generating points [6]. Both requirements can be fulfilled by the skeletonization based on Voronoi diagrams but it is regarded as an expensive process, especially for large and complex objects [21].

The *thinning* process is a frequently used method for producing an approximation to the skeleton in a *topology–preserving* way [14]. It is based on digital simulation of the fire front propagation: *border points* (i.e., object points that are "adjacent" to the background) of a binary object that satisfy certain topological and geometric constraints are deleted in iteration steps. The entire process is repeated until only the "skeleton" is left. The iterative process is shown in Figure 2. The topologically oriented thinning pays less attention to the metric properties of the object, therefore, the invariance under rotation (object orientation) is not guaranteed.

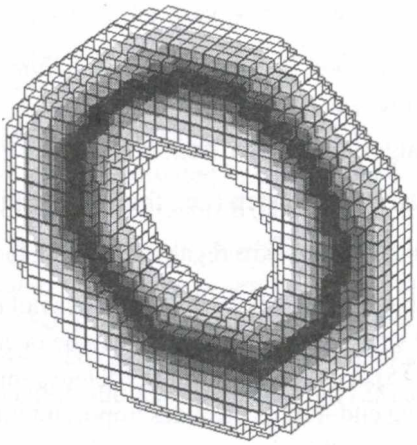

Figure 2. *Thinning of a doughnut–like 3D object. Results of the layer by layer deletion steps are denoted by different grey–levels. The darkest points belong to the "skeleton". (A point of a 3D binary picture can be modelled by a lattice point or by a unit cube. In this figure cubes represent points belonging to the actual object)*

We prefer thinning, since it:

— preserves topology;

— makes easy implementation possible (as a sequence of local Boolean operations);

— takes the least computational costs;

— can be executed in parallel.

2. Parallel thinning in 3D

A *3D binary picture* [14, 15] is a mapping that assigns the value of 0 or 1 to each point with integer coordinates in the 3D digital space denoted by $\mathbf{Z}^3$. Points having the value of 1 are called black points, while 0's are called white ones. Black points form *objects* of the picture. White points form the *background* and the *cavities* of the picture. Both the input and the output of a picture operation are pictures. Thinning is a picture operation which is regarded as a *reduction* (i.e., it can change some black points to white but white points remain the same). A thinning algorithm does *not* preserve topology [15] if:

— any object in the input picture is split (into two or more ones) or completely deleted,

— any cavity in the input picture is merged with the background or another cavity, or

— a cavity is created where there was none in the input picture.

There is an additional concept called a *hole* in 3D pictures. A hole (that doughnuts have) is formed by 0's, but it is not a cavity [14]. Topology preservation implies that eliminating or creating any hole is not allowed.

Each thinning algorithm can be sketched by the following program:

repeat
changing "deletable" border points to white
until *no points are deleted*

Existing 3D thinning algorithms differ from one another in two regards:

— How to organize an iteration step (i.e., the kernel of the **repeat** cycle)?

— Which types of border points are regarded as "deletable"?

A *simple point* is an object point whose deletion does not alter the topology of the picture [20]. Note that the simplicity of a 3D point can be decided by investigating its 3×3×3 neighborhood [14, 15]. Thinning algorithms delete simple points, which are not *end–points*, since preserving end–points provides important information relative to the shape of the objects. *Curve thinning* preserves *line end–points* while *surface thinning* does not delete *surface end–points* (see Figure 3).

Note that the Euclidean skeleton represents some kinds of *local object symmetries* [29]. The skeleton of a 3D object can contain some surface patches

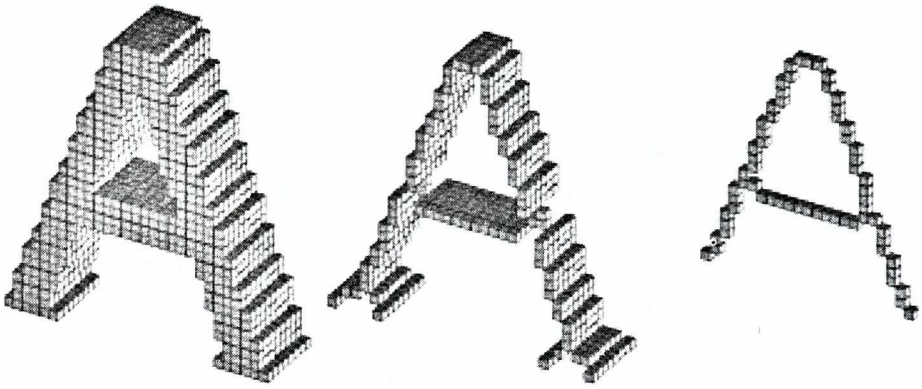

Figure 3. *A 3D synthetic object containing a character "A"(left); its medial surface (centre); its medial lines (right)*

(representing mirror symmetry and/or rotational symmetry) and some line segments (representing axial symmetry). The results of the surface thinning algorithms are closer to the 3D Euclidean skeleton than the "skeletons" produced by curve thinning algorithms. Axial symmetry is emphasized by curve thinning and other kinds of symmetries are suppressed. Extracting *curve skeleton* or *medial lines* is more relevant for a "tubular" object (e.g., blood vessels, some kinds of bones, and airway trees) than producing its *surface skeleton* or *medial surface.*

Most of the existing thinning algorithms are parallel, since the fire front propagation is by nature parallel. (This means that all border points satisfying the deletion condition of the actual phase of the process are simultaneously deleted.) Those algorithms delete a set of simple points that can alter the topology. Three methods have been proposed to overcome this problem:

1. Algorithms belonging to the first type do not divide an iteration step into subiterations [17–19]. In order to preserve topology, these *fully parallel* algorithms investigate some additional points that are in the 5×5×5 neighborhood but not in the 3×3×3 neighborhood.

2. The second type of algorithms examines the 3×3×3 neighborhood of each border point. Iteration steps are divided into a number of successive subiterations, where only border points of certain kind can be deleted in each subiteration. Consequently, each subiteration uses a different deletion rule. These algorithms are called *directional* or *border sequential* ones. Since there are six kinds of major directions in 3D images, six–subiteration directional thinning algorithms were generally proposed [2, 12, 16, 22, 31]. Note that Palágyi and Kuba have been proposed an eight–subiteration algorithm [24] and a twelve–subiteration one [25], too.

3. The third approach is the *subfield sequential* method. The set of points $\mathbf{Z}^3$ is divided into more disjoint subsets which are alternatively activated. At a given iteration step, only border points of the active subfield are designated to be

deleted. Two subfield sequential 3D thinning algorithms working in cubic grid have been proposed so far [1, 27]. Both algorithms use eight subfields. It is not by accident, since using those eight subfields ensures the topology preservation. Note that Palágyi and Kuba proposed a hybrid thinning algorithm using both subfield sequential and directional approaches [23].

The above three thinning methods are proposed to answer the first question: How to organize an iteration step of parallel thinning for providing topology preservation? The second important question is: Which types of black points are designated to be deleted? Some algorithms (in each phase) delete all simple points of a given type which are not end–points [1, 2, 16], others give the prescribed neighborhood of deletable points [12, 17, 18, 22–25, 27, 31]. Curve thinning (or medial line thinning) preserves line end–points while surface thinning (or medial surface thinning) does not delete surface end–points [16, 31]. Note that different surface end–point characterizations have been proposed by various authors [1,.2, 12, 16, 17, 31].

3. Skeletons in medical image processing

The importance of the skeleton as a region–based shape feature shows an upward tendency. Some important applications have I appeared in medical image processing, too.

Van den Elsen et al. [32] extracted ridge–like features in their medical image registration method. They used 3D thinning to eliminate unwanted thick ridges and blobs.

Various authors built distance maps from the extracted features in their registration methods [5, 13]. More accurate matching based on distance transformation can be reached if thinned feature data set is used. Thinning provides relevant information and reduces the feature search space of the geometric model to be evaluated.

Gerig et al. [11] used 3D thinning for symbolic description of cerebral vessel tree. Székely et al. [28] applied a 3D thinning algorithm for structural description of cerebral vascularity. Ma and Sonka [18] developed a 3D algorithm for thinning airway trees extracted from 3D CT studies.

Ge, Stelts and Vining [10] applied curve thinning for virtual colonoscopy. The resulting skeleton can be successfully used to guide the auto–piloting of virtual colonoscopy.

Näf et al. [21] proposed skeletons for the characterization and recognition of 3D organ shape. They illustrated the power of skeletal representation by two applications: bone thickness characterization (for optimal prosthesis placement in hip joint replacement operations) and generation of skeleton of a human brain (for analyzing its cortical structure).

A method has been published by Tari et al. [30] for extracting shape skeletons from (gray–scale) medical images.

Palágyi and Kuba have developed four different 3D thinning algorithms [22–25].

Note that the three directional ones [22, 24, 25] (using six, eight, and twelve subiterations, respectively) are capable of extracting both medial lines and medial surfaces. On the other hand, the foAAAh algorithm [23] was developed only for curve thinning.

Those algorithms have been tested for several synthetic and medical objects. Here we present two examples: both surface thinning and curve thinning of a human ventricle (Figure 4) and surface thinning of blood vessels of a human liver (Figure 5) are illustrated.

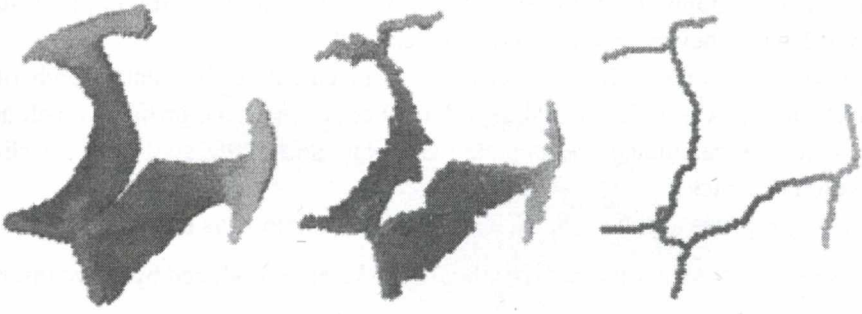

Figure 4. *Thinning of a human ventricle extracted from a (grey–scale) 3D MR brain study (left); the result of surface thinning (centre); the result of curve thinning (right). The skeletons were processed by the eight–subiteration directional algorithm [24]*

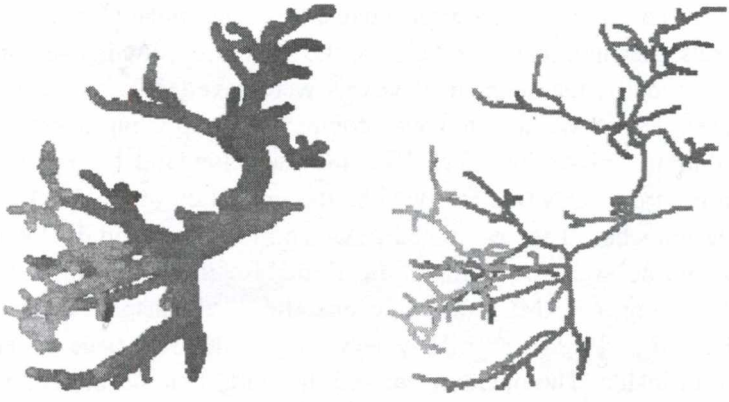

Figure 5. *Thinning of blood vessels of a human liver (left); the result of curve thinning (right). The skeleton was processed by the six–subiteration directional algorithm [22]*

4. Application to calculating cross–sectional profiles

Curve thinning can be used as in our example for calculating the central path within a prior segmented tubular structure: for calculating cross–sectional profiles in order to quantify narrowing in vessels or airways inter–observer of physicians up to 50/path planning of virtual endoscopy [26].

We used the cross–sectional profile in patients suffering from infra–renal aortic aneurysms (AAA). AAA are abnormal dilatations of the main arterial abdominal vessel due to atherosclerosis. AAA can be found in 2% of people older than 60 years. If the diameter is more than 5 cm, then the person is at high risk for AAA rupture, which leads to death in 70–90% of cases. For therapy two main options exist: surgery or endoluminal repair with stentgrafts. For optimal patient management the AAA extent regarding the "true diameter" as well as the distance to the renal arteries and the aortic bifurcation have to be known.

For imaging of AAA different imaging modalities can be used, most often Spiral Computed Tomography (S–CT). Since these AAA extend in any direction of 3D, an axial S–CT slices never "true diameter" is depicted.

Applying thinning to S–CT slices allows to calculate the central path of the abdominal aorta. Along the medial axis the 3D cross–sectional profile as well as the 3D diameter are calculated and depicted as a line chart, where all relevant clinical information is depicted.

The major phases of the proposed method are described as follows:

— segmentation, computation of the AAA skeleton produced by curve thinning;

— separation of the AAA central path from that skeleton;

— smoothing of the AAA central path and calculation of the AAA crossectional profile orthogonal to the central path.

AAA segmentation was performed by an in house developed semiautomated software using snakes. The segmented voxels were interpolated in order to obtain isotropic voxels, meaning that all voxels had the same extension in every direction of the 3D space. Finally, the segmented voxels were saved as a binary volume (3D binary picture). The AAA skeleton was computed by applying a six–subiteration directional thinning algorithm [22]. The raw skeleton and its medial path are illustrated in Figure 6. This was followed by the separation of the AAA central path from the side branches. The segmented AAA and the computed 3D skeleton were converted according to the standards of the Virtual Reality Modelling Language 2.0 (VRML) [8]. Using a VRML editor the operator could inspect interactively the trachea and the 3D skeleton from any view within the 3D space — either from outside or from inside. The operator marked the startpoint and the endpoint of the central path with a color different to that of the remaining 3D skeleton. Afterwards the shortest path in the skeleton between the startpoint and endpoint was computed using a shortest–path searching algorithm [9]. The determined central path was represented by a sequence of vectors from the starting point to the endpoint. Those vectors formed a zigzag line. The smoothing method connected the middle point of each vector. 100 iterations of this algorithm produced a sufficient straight medial axis. Figure 7 demonstrates a virutal angioscopic view with the calculated AAA central path. Orthogonal to the AAA medial axis the cross–sectional area was calculated from the interpolated data volume, which represented the segmented AAA. Finally a line chart was drawn, where for every point of the AAA medial

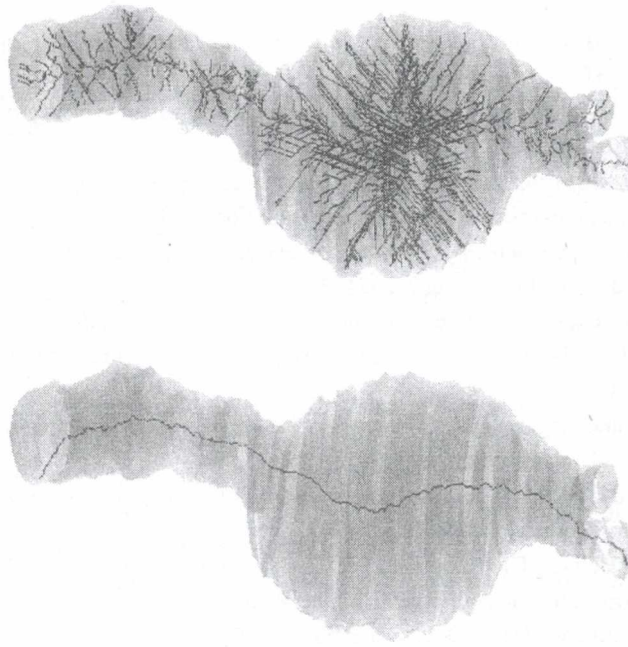

Figure 6. *Raw skeleton as a result of the applied curve thinning (top) and the determined central path (bottom). (The skeletal parts are superimposed to the original object)*

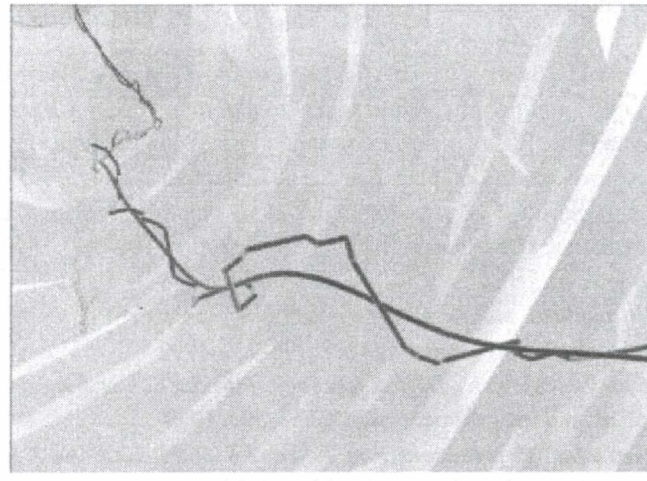

Figure 7. *Corresponding parts of the original central path and the smoothed one*

axis, the crossectional area was plotted against the distance in 3D to the vocal cords. The positions of the stored anatomic landmarks were automatically marked on the charts.

Acknowledgements

This work was supported by OTKA T023804 and CEEPUS A–34 Grants.

References

[1] Bertrand G. and Aktouf Z., *A 3D thinning algorithms using subfields*, in Proc. SPIE Conf. on Vision Geometry III 2356, 113–124, 1994

[2] Bertrand G., *A parallel thinning algorithm for medial surfaces*, Pattern Recognition Letters 16, 979–986, 1995

[3] Blum H., *A transformation for extracting new descriptors of shape*, Symposium on Models for the perception of Speech and Visual Form, 1964

[4] Borgefors G., *Distance transformations in arbitrary dimensions*, Computer Vision, Graphics, and Image Processing 27, 321–345, 1984

[5] Borgefors G., *Hierarchical chamfer matching: A parametric edge matching algorithm*, IEEE Transactions on Pattern Analysis and Machine Intelligence 10, 849–865, 1988

[6] Brandt J.W. and Algazi V.R., *Continuous skeleton computation by Voronoi diagram*, CVGIP: Image Understanding 55, 329–338, 1992

[7] Calabi L. and Hartnett W.E., *Shape recognition, prairie fires, convex deficiencies and skeletons*, Am. Math. Monthly 75, 335–342, 1968

[8] Carey R. and Bell G., The Annotated VRML 2.0 Reference Manual, in The VRML 2.0 Handbook: Building Moving Worlds on the Web, Eds.: Hartmann J., Wernecke J., Carey R., Addison–Wesley Devekopers Press, 197, 1996

[9] Corman T.H., Leiserson C.E. and Rivest R.L., *Introduction to Algorithms*, MIT Press, 1993

[10] Ge Y., Stelts D.R. and Vining D.J., *3D skeleton for virtual colonoscopy*, in Proc. 4th Int. Conf. Visualization in Biomedical Computing, VBC'96, Lecture Notes in Computer Science 1131, Springer, 449–454, 1996

[11] Gerig G., Koller Th., Székely G., Brechbühler Ch. and Kübler O., *Symbolic description of 3–D structures applied to cerebral vessel tree obtained from MR angiography volume data*, in Proc. 13th Int. Conf. Information Processing in Medical Imaging, IPMI'93, Lecture Notes in Computer Science 687, Springer–Verlag, 94–111, 1993

[12] Gong W.X. and Bertrand G., *A simple parallel 3D thinning algorithm*, in Proceedings 10th IEEE International Conference on Pattern Recognition, 188–190, 1990

[13] Jiang H., Robb A. and Holton K.S., *A new approach to 3–D registration of multimodality medical images by surface matching*, in Proc. SPIE Conf. on Visualization in biomedical computing 1808, 196–213, 1992

[14] Kong T.Y. and Rosenfeld A., *Digital topology: Introduction and survey*, Computer Vision, Graphics, and Image Processing 48, 357–393, 1989

[15] Kong T.Y., *On topology preservation in 2–D and 3–D thinning*, Int. J. of Pattern Recognition and Artifical Intelligence 9, 813–844, 1995

[16] Lee T., Kashyap R.L. and Chu C., *Building skeleton models via 3–D medial surface/ axis thinning algorithms*, CVGIP: Graphical Models and Image Processing 56, 462–478, 1994

[17] Ma C.M., *A 3D fully parallel thinning algorithm for generating medial faces*, Pattern Recognition Letters 16, 83–87, 1995

[18] Ma C.M. and Sonka M., A *fully parallel 3D thinning algorithm and its applications*, Computer Vision and Image Understanding 64, 420–433, 1996

[19] Manzanera A., Bernard T.M., Preteux F. and Longuet B., *Medial faces from a concise 3D thinning algorithm*, in Proc. 7th IEEE Int. Conf. on Computer Vision, ICCV'99, 1999, to appear

[20] Morgenthaler D.G., *Three-dimensional simple points: Serial erosion, parallel thinning and skeletonization*, TR-1005, Computer Vision Laboratory, Computer Science Center, Univ. of Maryland, College Park, MD., 1981

[21] Näf M., Székely G., Kikinis R., Shenton M.E. and Kübler G., *3D Voronoi skeletons and their usage for the characterization and recognition of 3D organ shape*, Computer Vision, Graphics, and Image Processing 66, 147–161, 1997

[22] Palágyi K. and Kuba A., *A 3D 6-subiteration thinning algorithm for extracting medial lines*, Pattern Recognition Letters 19, 613–627, 1998

[23] Palágyi K. and Kuba A., *A hybrid thinning algorithm for 3D medical images*, Journal of Computing and Information Technology 6, 149–164, 1998

[24] Palágyi K. and Kuba A., *Directional 3D thinning using 8 subiterations*, in Proc. 8th Int. Conf. on Discrete Geometry for Computer Imagery, DGCI'99, Lecture Notes in Computer Science 1568, Springer, 325–336, 1999

[25] Palágyi K. and Kuba A., *A parallel 3D 12-subiteration thinning algorithm*, Graphical Models and Image Processing 61, 199–221, 1999

[26] Rubin P. and Johnston N., *Measurement of the Aorta and Its Branches with Helical CT*, Radiology 206, 823–829, 1998

[27] Saha P.K., Chaudhury B.B. and Majumder D.D., *A new shape-preserving parallel thinning algorithm for 3D digital images*, Pattern Recognition 30, 1939–1955, 1997

[28] Székely G., Koller Th., Kikinis R. and Gerig G., *Structural description and combined 3-D display for superior analysis of cerebral vascularity from MRA*, in Medical Imaging: Analysis of multimodality 2D/3D images, IOS Press, 183–194, 1995

[29] Székely G., *Shape characterization by local symmetries*, Habilitationsschrift, Institute for Communication Technology, Image Science Division, ETH Zürich, 1996

[30] Tari S., Shah J. and Pien H., *Extraction of shape skeletons from grayscale images*, Computer Vision and Image Understanding 66, 133–146, 1997

[31] Tsao Y.F. and Fu K.S., *A parallel thinning algorithm for 3-D pictures*, Computer Graphics and Image Processing 17, 315–331, 1981

[32] Van den Elsen P.A., Maintz J.B.A., Pol E.J.D. and Viergever M.A., *Image fusion using geometrical features*, in Proc. SPIE Conf. on Visualization in biomedical computing 1808, 172–186, 1992